
¹⁸F-Branched-Chain Amino Acids: Structure–Activity Relationships and PET Imaging Potential

Matthew B. Nodwell¹, Hua Yang², Helen Merckens^{3,4}, Noeen Malik^{2,3}, Milena Čolović^{3,4}, Björn Wagner⁵, Rainer E. Martin⁶, François Bénard^{3,4}, Paul Schaffer^{1,2,4}, and Robert Britton¹

¹Department of Chemistry, Simon Fraser University, Burnaby, British Columbia, Canada; ²Life Sciences Division, TRIUMF, Vancouver, British Columbia, Canada; ³Department of Molecular Oncology, BC Cancer Agency, Vancouver, British Columbia, Canada; ⁴Department of Radiology, University of British Columbia, Vancouver, British Columbia, Canada; ⁵Pharmaceutical Sciences, Roche Pharma Research and Early Development, Roche Innovation Center Basel, F. Hoffmann-La Roche Ltd., Basel, Switzerland; and ⁶Medicinal Chemistry, Roche Pharma Research and Early Development, Roche Innovation Center Basel, F. Hoffmann-La Roche Ltd., Basel, Switzerland

The large, neutral L-type amino acid transporters (LAT1–LAT4) are sodium-independent transporters that are widely distributed throughout the body. LAT expression levels are increased in many types of cancer, and their expression increases as cancers progress, leading to high expression levels in high-grade tumors and metastases. Because of the key role and overexpression of LAT in many types of cancer, radiolabeled LAT substrates are promising candidates for nuclear imaging of malignancies that are not well revealed by conventional radiotracers. The goal of this study was to examine the structure–activity relationships of a series of ¹⁸F-labeled amino acids that were predicted to be substrates of the LAT transport system. **Methods:** Using a photocatalytic radical fluorination, we prepared a series of 11 fluorinated branched-chain amino acids and evaluated them and their nonfluorinated parents in a cell-based LAT affinity assay. We radiofluorinated selected branched-chain amino acids via the same radical fluorination reaction and evaluated tumor uptake in U-87 glioma xenograft-bearing mice. **Results:** Structure–activity relationship trends observed in a LAT affinity assay were maintained in further *in vitro* studies, as well as *in vivo* using a U-87 xenograft model. LAT1 uptake was tolerant of fluorinated amino acid stereochemistry and chain length. PET imaging and biodistribution studies showed that the tracer (S)-5-¹⁸F-fluorohomoleucine had rapid tumor uptake, favorable *in vivo* kinetics, and good stability. **Conclusion:** By using an *in vitro* affinity assay, we could predict LAT-mediated cancer cell uptake in a panel of fluorinated amino acids. These predictions were consistent when applied to different cell lines and murine tumor models, and several new tracers may be suitable for further development as oncologic PET imaging agents.

Key Words: LAT transport; ¹⁸F radical fluorination; structure–activity relationships

J Nucl Med 2019; 60:1003–1009

DOI: 10.2967/jnumed.118.220483

A hallmark of cancer is a metabolic reprogramming of cells that enables increased nutrient uptake and altered metabolism required for rapid growth and division (1). In addition to the increased uptake of glucose by cancer cells, most malignancies also display an increased uptake of amino acids that are required for accelerated protein synthesis, alternative modes of energy production, or cell signaling (2). Because amino acids have traditionally shown low basal uptake in tissues with high glucose uptake such as brain, inflammation, or infection, ¹⁸F-amino acid radiotracers can complement ¹⁸F-FDG PET imaging in the visualization and quantification of various malignancies (3). Of interest to cancer biology are the L-type amino acid transporters (LATs) and, more specifically, LAT1, which plays a key role in transporting large, neutral amino acids (4,5). LAT1 is overexpressed in a wide variety of human tumors, and its expression level correlates with tumor cell proliferation, angiogenesis, and poor patient outcomes (6). Thus, LAT1 represents a promising target for cancer imaging via PET. In particular, PET radiotracers targeted toward the LAT system are of value in the imaging and monitoring of gliomas because LAT is highly expressed at the blood–brain barrier (BBB), thus supplying the brain with essential amino acids (7). This expression at the BBB allows LAT-targeted radiotracers to reach the entire brain volume, as well as glioblastomas with intact BBB membranes (8). The key role that LAT transport plays in both cancer and BBB crossing renders the study and discovery of LAT-targeting amino acid radiotracers a valuable medical endeavor.

To date, several amino acid LAT substrates have displayed promise as oncologic PET tracers (Fig. 1). Most of these are α -hydrogen- α -amino acids, have an (S) stereochemical configuration, and contain an aromatic ring. Tracers such as *O*-(2-¹⁸F-fluoroethyl)-L-tyrosine (¹⁸F-FET) (9) and 6-¹⁸F-fluoro-3,4-dihydroxy-L-pheynylalanine (¹⁸F-FDOPA) (10) have been used for imaging of various cancers in humans and are particularly useful for neurooncologic imaging (11,12). In the case of aromatic LAT substrates, replacement of the α -hydrogen with a methyl group, as in L-3-¹⁸F-fluoro- α -methyl tyrosine (¹⁸F-FAMT) (13) and 3-¹²³I-iodo- α -methyl-L-tyrosine (¹²³I-IMT) (14), does not appear to affect LAT affinity and, in the case of ¹⁸F-FAMT, can impart selectivity for LAT1 over LAT2 (15). Aliphatic radiolabeled LAT substrates include L-¹¹C-methionine (¹¹C-MET) (16), (S)-2-amino-7-¹⁸F-fluoroheptanoic acid ((S)-¹⁸F-FAHep) (17), and (S)-5-¹⁸F-fluoroleucine (18). Of these, only ¹¹C-MET has

Received Sep. 17, 2018; revision accepted Nov. 30, 2018.

For correspondence or reprints contact: Robert Britton, Department of Chemistry, Simon Fraser University, 8888 University Dr., Burnaby BC Canada V5A 1S6.

E-mail: rbritton@sfu.ca

Published online Jan. 25, 2019.

COPYRIGHT © 2019 by the Society of Nuclear Medicine and Molecular Imaging.

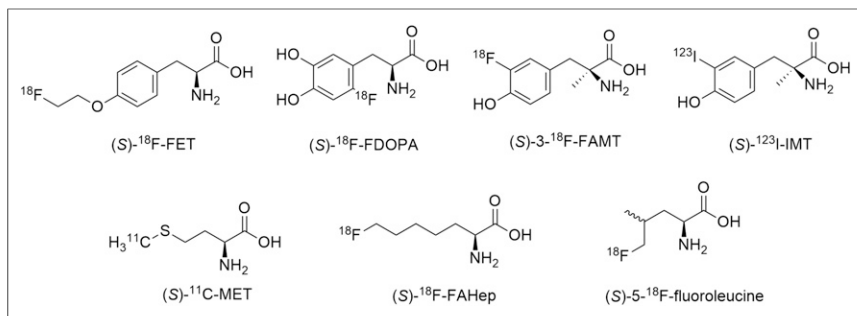


FIGURE 1. Radiolabeled amino acid tracers targeting LAT.

been used in humans, and although (S)-¹⁸F-FAHep shows promise for brain tumor imaging, (S)-5-¹⁸F-fluoroleucine shows significant *in vivo* defluorination, limiting its further development. Despite these and other discoveries, the number of systematic structure–activity relationship (SAR) studies related to LAT-based radiotracers remains limited. A recent study by Nagamori et al. indicates that a β-amino acid (L-β-homoleucine) and D-amino acids (D-leucine, and D-homoleucine) can act as effective LAT substrates, yet these findings have not been translated to *in vivo* radiotracer studies (19). Bouhrel et al. have also reported in select cases that (R)-configured amino acids display LAT-mediated transport (20). Furthermore, although any amino acid radiotracer can potentially be synthesized by labeling the carboxylate terminus with ¹¹C, yielding an unsubstituted amino acid (21), a formal comparison of unsubstituted versus fluorinated amino acids in cellular amino acid transport has, to the best of our knowledge, not yet been performed. As with drug discovery, SAR can be a powerful tool in the rational design of optimized radiotracers, and in the current study, we apply a SAR approach to the study of LAT substrates and their potential as oncologic radiotracers.

We recently reported the radiosynthesis of several ¹⁸F-labeled branched-chain amino acids (¹⁸F-FBCAAs) via a photocatalyzed radical fluorination (22). Here, we use this fluorination platform to synthesize an extended panel of ¹⁸F-labeled BCAAs. Evaluation of the LAT-mediated transport of these BCAAs and their potential

as tumor imaging agents was performed by both *in vitro* and *in vivo* methods. We find that the major transporter responsible for ¹⁸F-FBCAA uptake is the LAT system and that LAT affinity correlates with the ability of the ¹⁸F-FBCAAs to be taken up in U-87 xenograft tumors.

MATERIALS AND METHODS

Radiosynthesis

¹⁸F-F₂ was generated from a TR13 cyclotron by a 2-part irradiation process. ¹⁸O-O₂/Ar was loaded to the target chamber and irradiated at 25 μA/min for 15 min. ¹⁸O-O₂ was trapped cryogenically and recycled. Then, the target was filled with F₂/argon and irradiated again at 20 μA/min for 5 min. The target was emptied to the synthesis module by an argon flow. The ¹⁸F-FBCAAs were radiosynthesized in a manner similar to that previously described (22). Briefly, ¹⁸F-F₂ was bubbled through a solution of sodium dibenzenesulfonamide (40 mg) in 600 μL of CH₃CN and 200 μL of H₂O. The reaction mixture was loaded on a C18 long SepPak (WAT023635; Waters). After washing with 5 mL of H₂O and 0.6 mL of CH₃CN, ¹⁸F-N-fluorobenzenesulfonimide (NFSI) was eluted with 1.2 mL of CH₃CN. The ¹⁸F-NFSI solution was added to a slurry of the substrate as a trifluoroacetic acid salt (typically 10–15 mg) and sodium decatungstate (5 mg, 2.0 μmol) in 200–400 μL of H₂O and mixed briefly. The solution was then loaded onto a microfluidic reactor (XXL-ST-02; Little Things Factory) on a transilluminator (89131-468, 365 nm; VWR) shown in Supplemental Figure 1 (supplemental materials are available at <http://jnm.snmjournals.org>) and photoirradiated for 45 min. After this time, the solution was removed and the photoreactor was washed with CH₃CN (5 mL). The resulting solution was loaded onto a strong cation-exchange cartridge (500 mg of resin, SPE-P0005; SiliCycle), and the cartridge was washed with CH₃CN (10 mL) followed by H₂O (10 mL). The ¹⁸F-FBCAAs were then eluted from the cartridge with 1 mL aliquots of 150 mM NaHCO₃, yielding a mixture of fluorinated product and starting material. Analytic high-performance liquid chromatography was performed on a Phenomenex Luna C18 (4.6 × 150 mm, 1 mL/min)

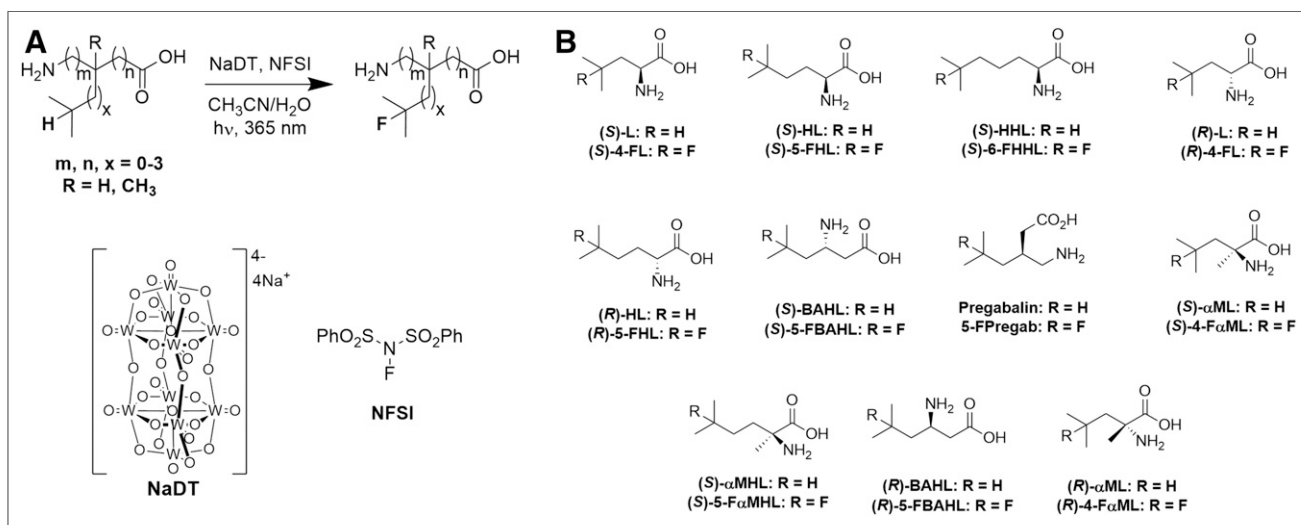


FIGURE 2. (A) Direct fluorination of BCAAs using photochemical radical fluorination. (B) Panel of 22 parent and fluorinated BCAAs used in this study.

using a gradient of 100% solvent A (0.1% trifluoroacetic acid in H₂O) to 100% solvent B (0.1% trifluoroacetic acid in CH₃CN) over 15 min.

RESULTS

Chemistry

When necessary, resolution was performed by a 2-step *N*-acylation and enzymatic deacylation using porcine kidney acylase to yield the (*S*)-isomer of the BCAA according to Chenault et al. (23). The BCAAs were fluorinated via a photocatalytic C-H fluorination procedure (24–26) as depicted below (Fig. 2) and described in the supplemental materials.

LAT Uptake Studies

To quantify the ability of the BCAAs to be transported by the LAT system, a leucine transport assay was used, which measures the antagonism of ³H-leucine uptake in CHO-K1 cells (4). The results from this study (Fig. 3) add to the work of Nagamori et al., who previously performed LAT transport SAR in HeLa S3 cells, albeit at a single concentration (1 mM) (19). We found that LAT transport was optimal for α -amino acids and that a 1-carbon increase in aliphatic chain length was tolerated (Fig. 3, entries 1–3). In line with results reported by Nagamori et al. (19), we found that LAT was relatively tolerant of the absolute stereochemistry of α -amino acids, with similar LAT affinity for both enantiomers (Fig. 3, entries 1, 2, 4, and 5). However, we found a clear difference in LAT affinity between enantiomeric β -amino acids (Fig. 3, entries 6 and 10). Notably, fluorination of the BCAAs at the branched position did not greatly affect LAT affinity for optimal substrates but decreased affinity in poorer substrates (Fig. 3, entries 6, 7, and 8). In accord with findings reported by Bouhrel et al. (17), we found that α -methylation greatly diminished LAT affinity (Fig. 3, entries 8 and 9). These findings confirm that α -methylation in aliphatic amino acids, as opposed to aromatic amino acids, decreases LAT affinity and that the use of the more desirable ¹⁸F radiolabel, as opposed to ¹¹C, should not impair LAT transport for higher-affinity LAT substrates.

The structure of mammalian LAT1 is as yet unknown; however, homology modeling based on the x-ray structure of the arginine/ agmatine transporter AdiC from *Escherichia coli* displays crucial substrate binding via hydrogen bonds at the acid oxygens and amino group (27). To shed light on the effect of fluorination on the BCAAs, we measured the pK_a of 3 BCAA/FBCAA couples: (*S*)-HL/(*S*)-5-fluorohomoleucine (FHL), pregabalin/5-FPregab, and (*S*)- α MHL/(*S*)-5-F α MHL (Fig. 4). In all cases, fluorination lowered the pK_a values of the acid and base slightly. Although the effect of fluorination on ammonium pK_a was relatively constant among the compounds analyzed (Δ pK_a \sim -0.40), fluorination decreased the pK_a of the carboxylic acid function by about 0.1 for pregabalin and (*S*)- α MHL but had almost no effect (Δ pK_a \sim -0.03) for (*S*)-HL. The difference between carboxylic acid pK_a for pregabalin and 5-FPregab may contribute to the decrease in LAT affinity for 5-FPregab, which was not observed between (*S*)-HL and (*S*)-5-FHL.

Radiosynthesis

The 2-step radiosynthesis of ¹⁸F-FBCAAs was adapted from our previous report (22). First, ¹⁸F-NFSI (28) was produced by passing ¹⁸F-F₂ through the CH₃CN-H₂O solution of sodium dibenzene-sulfonamide. This was followed by loading a mixture of BCAA, sodium decatungstate, and ¹⁸F-NFSI in CH₃CN-H₂O solution onto a microfluidic reactor placed on a transilluminator and irradiated

Entry	Structure	LAT IC ₅₀ (μ M)	
		R = H	R = F
1	 (<i>S</i>)-L, (<i>S</i>)-4-FL	9.15 \pm 1.1	7.17 \pm 1.6
2	 (<i>S</i>)-HL, (<i>S</i>)-5-FHL	3.75 \pm 0.40	5.30 \pm 0.82
3	 (<i>S</i>)-HHL, (<i>S</i>)-6-FHHL	14.1 \pm 5.6	16.6 \pm 2.9
4	 (<i>R</i>)-L, (<i>R</i>)-4-FL	17.4 \pm 3.9	23.6 \pm 6.0
5	 (<i>R</i>)-HL, (<i>R</i>)-5-FHL	22.0 \pm 6.7	26.0 \pm 6.3
6	 (<i>S</i>)-BAHL, (<i>S</i>)-5-FBAHL	155 \pm 28	395 \pm 128
7	 Pregabalin, 5-FPregab	188 \pm 53	>1000
8	 (<i>S</i>)- α ML, (<i>S</i>)-4-F α ML	387 \pm 112	>1000
9	 (<i>S</i>)- α MHL, (<i>S</i>)-5-F α MHL	>1000	>1000
10	 (<i>R</i>)-BAHL, (<i>R</i>)-5-FBAHL	>1000	>1000
11	 (<i>R</i>)- α ML, (<i>R</i>)-4-F α ML	>1000	>1000

FIGURE 3. LAT affinity of BCAA/FBCAA pairs in CHO cells. IC₅₀ is for uptake of ³H-leucine into CHO-K1 cells in Na⁺-free medium.

at a λ of 365 nm at ambient temperature for 45 min. Purification was performed via a cation-exchange cartridge. In all cases, the ¹⁸F-FBCAAs were synthesized and purified in less than 60 min. The radiochemical parameters of the ¹⁸F-FBCAAs are shown in Figure 5. The use of ¹⁸F-F₂ gas results in radiotracers with low molar activities (\sim 3–16 MBq/ μ mol), and although this may not be suitable for all purposes, fluorinated amino acid radiotracers of this molar activity range have previously been effective in clinical studies (29).

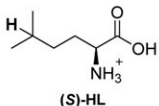
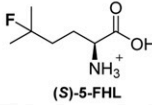
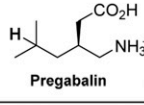
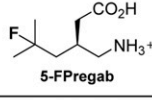
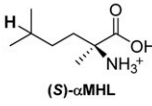
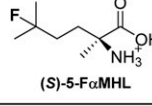
Entry	Structure	pKa Acid	pKa Base
1	 (S)-HL	2.30	9.66
2	 (S)-5-FHL	2.27	9.28
3	 Pregabalin	3.98	10.20
4	 5-FPregab	3.86	9.79
5	 (S)-αMHL	2.30	10.00
6	 (S)-5-FαMHL	2.16	9.62

FIGURE 4. Measured pKa values for selected BCAA/FBCAA pairs. pKa acid = carboxylic acid; pKa base = protonated amine.

Competition Assay

We further examined the uptake of a selected panel of 5 ¹⁸F-FBCAAs in a PSMA (prostate specific membrane antigen)-negative prostate cancer cell line (PC3). Uptake of the ¹⁸F-FBCAAs was measured with or without the addition of a competitive amino acid substrate to interrogate the specificity of FBCAA uptake. Here, the uptake of all 5 tracers was blocked by L-leucine and 2-amino[2.2.1]heptane-2-carboxylic acid (BCH), which are

LAT-specific inhibitors (30). The uptake was not blocked by L-glutamate, L-serine, or N-methyl α-aminoisobutyric acid, indicating that these new tracers are not transported by excitatory amino acid transporters, system xCT, system A, or system ASC (31). Uptake of each tracer was blocked to a similar extent by BCH and L-leucine, indicating a similar role of LAT in their transport. Conversely, transport of (S)- and (R)-5-¹⁸F-FHL was not affected by excess L-phenylalanine, which largely inhibited uptake of the other ¹⁸F-FBCAAs, indicating a contribution of the other transport systems to the uptake of these radiotracers (Fig. 6). Notably, uptake in PC3 cells was the highest for (S)-5-¹⁸F-FHL, followed by (R)-5-¹⁸F-FHL, (S)-5-¹⁸F-FBAHL, (R)-5-¹⁸F-FBAHL, and (S)-4-¹⁸F-FαML, in agreement with the data presented in Figure 3.

In Vivo Biodistribution

We elected to further study the LAT-based tumor uptake of a panel of ¹⁸F-FBCAAs in NSG (NOD Scid gamma) mice xenografted with U-87 tumors based on our *in vitro* data. As would be expected from amino acid radiotracers, accumulation was pronounced in the pancreas and kidney, with excretion mainly via the urine (Fig. 7, Supplemental Table 1). All compounds displayed good metabolic stability as evidenced by low bone uptake, with the exception of 5-¹⁸F-FPregab, which displayed slightly elevated bone accumulation (3.36 ± 0.55 percentage injected dose [%ID]/g). (S)-5-¹⁸F-FHL, (S)-6-¹⁸F-FHHL, and (R)-5-¹⁸F-FHL had higher tumor uptake than (S)-5-¹⁸F-FBAHL. 5-¹⁸F-FPregab, (S)-4-¹⁸F-FαML, and (S)-5-¹⁸F-FαMHL had much lower tumor uptake. These results were consistent with our findings in cell uptake assays. (S)-5-¹⁸F-FHL, (S)-6-¹⁸F-FHHL, and (R)-5-¹⁸F-FHL displayed brain uptake comparable to that of (S)-5-¹⁸F-FBAHL, 5-¹⁸F-FPregab, (S)-4-¹⁸F-FαML, and (S)-5-¹⁸F-FαMHL, consistent with LAT expression patterns at the BBB (7).

DISCUSSION

The LAT family is responsible for the transport of large, neutral amino acids such as phenylalanine, leucine, and isoleucine (4). Among the LAT family, LAT1 is the most extensively overexpressed in many types of tumors and their metastatic lesions, with expression of LAT1 correlating with tumor cell proliferation, angiogenesis, and poor prognosis (32). The overexpression of LAT1 and other members of the LAT transporter family in cancers and the resulting accumulation of neutral, hydrophobic amino acids

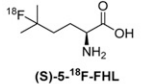
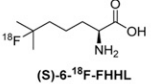
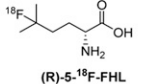
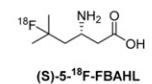
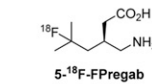
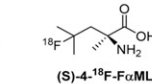
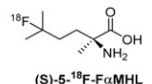
	 (S)-5- ¹⁸ F-FHL	 (S)-6- ¹⁸ F-FHHL	 (R)-5- ¹⁸ F-FHL	 (S)-5- ¹⁸ F-FBAHL	 5- ¹⁸ F-FPregab	 (S)-4- ¹⁸ F-FαML	 (S)-5- ¹⁸ F-FαMHL
RCY	27.9 ± 3.3 % ^a	15.4 ± 1.5 %	27.9 ± 3.3 % ^a	29.8 ± 0.7 % ^a	20.8 ± 7.3 %	20.1 ± 3.0 %	28.8 ± 1.7 %
RCP	> 97 %	> 95 %	> 97 %	> 97 %	> 97 %	> 97 %	> 97 %
MA (MBq/μmol)	6.3 ± 0.9 ^a	10.5 ± 1.3	6.3 ± 0.9 ^a	2.6 ± 0.6 ^a	15.6 ± 3.9	8.9 ± 0.8	11.8 ± 1.0

FIGURE 5. Radiochemical parameters for radiosynthesis of ¹⁸F-FBCAAs evaluated *in vivo* in this study. All numbers are $n = 3$ or greater, with exception of (S)-6-¹⁸F-FHHL, which was synthesized with $n = 2$. ^aPreviously reported (22). RCY = radiochemical yield of isolated final products from ¹⁸F-NFSI → ¹⁸F-FBCAA transformation; RCP = radiochemical purity as determined by radiodetected reversed-phase high-performance liquid chromatography; MA = molar activity in MBq/μmol as determined by ¹H NMR spectroscopy (more detail is in supplemental materials).

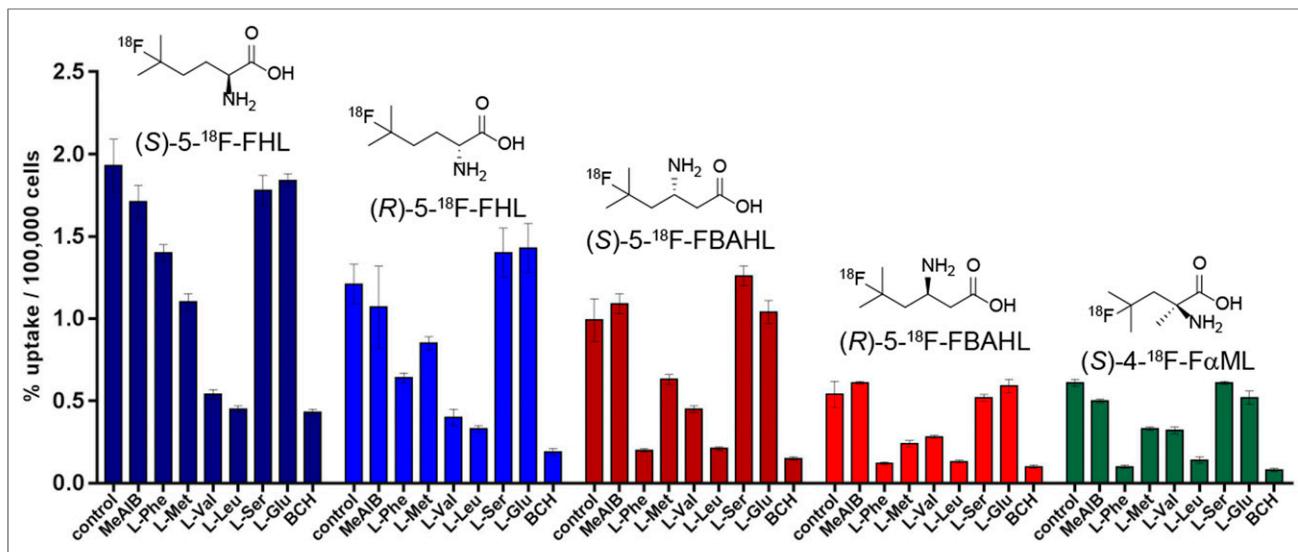


FIGURE 6. *In vitro* uptake of (S)-5-¹⁸F-FHL, (S)-5-¹⁸F-FBAHL, (S)-4-¹⁸F-FαML, (R)-5-¹⁸F-FHL, and (R)-5-¹⁸F-FBAHL in PC3 prostate cancer cells in presence of competitive inhibitors (10 mM) of amino acid transport. Uptake data are expressed as percentage relative to control condition (no competition), and values are normalized to total numbers of cells per well. MeAIB = *N*-methyl α-aminoisobutyric acid.

makes the use of ¹⁸F-labeled leucine-based radiotracers an attractive approach to PET imaging in oncology.

In this report, we applied a photocatalytic fluorination reaction (24,25,33) to rapidly produce and evaluate a series of fluorinated BCAAs as PET radiotracers. *In vitro* LAT affinity measured in CHO-K1 cells (Fig. 3) demonstrated a fair degree of substrate

promiscuity because both (S)- and (R)-α-amino acids were well transported into cells. Indeed, both stereoisomers of leucine and HL displayed similar LAT affinity in our system (half-maximal inhibitory concentration [IC₅₀] ~ 15 μM). β-amino acids were less ideal substrates, as (S)-BAHL displayed approximately an order of magnitude poorer affinity (IC₅₀ ~ 150 μM) toward LAT than

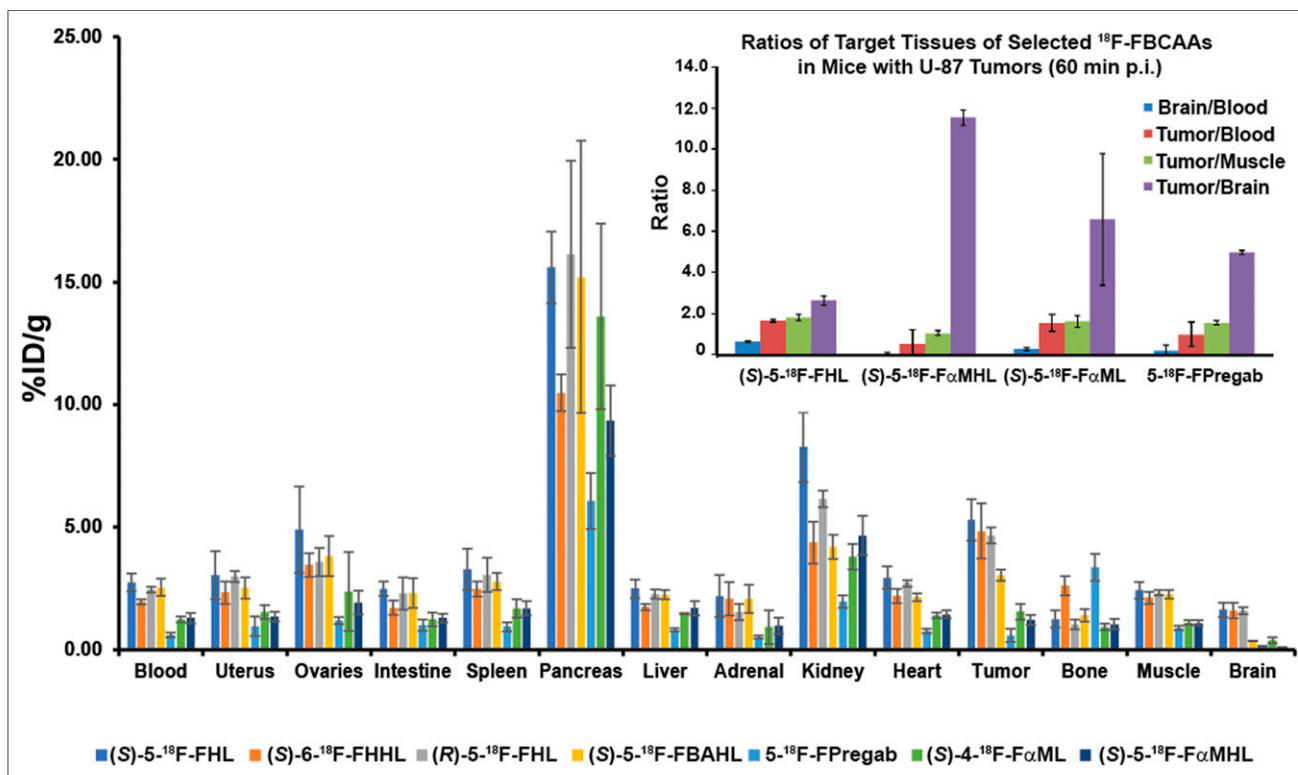


FIGURE 7. *In vivo* biodistribution in NSG mice bearing U-87 xenograft tumors with (S)-5-¹⁸F-FHL, (S)-6-¹⁸F-FHHL, (R)-5-¹⁸F-FHL, (S)-5-¹⁸F-FBAHL, (S)-5-¹⁸F-FPregab, (S)-4-¹⁸F-FαML, and (S)-5-¹⁸F-FαMHL, and ratios of selected tracer uptake in target tissues (inset). All data were obtained 60 min after injection. Data are %ID/g (mean ± SD, *n* ≥ 3).

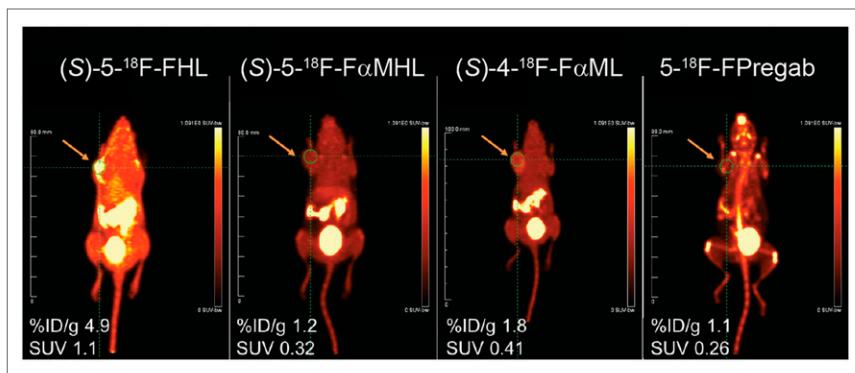


FIGURE 8. PET images at 10 min for U-87 xenograft-bearing mice with (S)-5-¹⁸F-FHL, (S)-5-¹⁸F-FαMHL, (S)-4-¹⁸F-FαML, and 5-¹⁸F-FPregab. The orange arrow indicates the site of tumor.

either (S)- or (R)-HL, and (R)-BAHL displayed little LAT affinity ($IC_{50} > 1,000 \mu M$). Longer chains were tolerated, as (S)-HHL was transported to approximately the same extent as the leucine and HL series. We found that α -methylation resulted in a significant decrease in LAT affinity, with αML ($IC_{50} \sim 400 \mu M$) and αMHL ($IC_{50} > 1000 \mu M$) in line with previous studies (17). Fluorination at the branched position in these amino acids resulted in negligible changes in LAT affinity for well-accepted substrates (L, HL, HHL) but was less tolerated in moderate substrates (BAHL, αML , αMHL). The central nervous system amino acid drug pregabalin (34), which is carried past the BBB via LAT transport, displayed an IC_{50} of about $190 \mu M$, in good agreement with a previous report (35). However, fluorination of this substrate to afford 5-FPregab resulted in complete loss of LAT affinity.

Radiofluorination provided ¹⁸F-FBCAAs in good radiochemical yield and purity, and *in vitro* uptake of these radiolabeled amino acids was examined in a PSMA-negative prostate cancer cell line (PC3). In this assay, we found that radiotracer uptake correlated with findings from the LAT affinity assay. We further showed that the uptake was efficiently blocked by BCH, L-valine, L-leucine, and, to a lesser extent, L-Met but not by *N*-methyl α -aminoisobutyric acid, L-Ser, or L-Glu, indicating that the primary *in vitro* uptake mechanism of these ¹⁸F-FBCAAs was via the L-type

system. In the case of poorer LAT substrates such as (S)-5-¹⁸F-FBAHL, (R)-5-¹⁸F-FBAHL, and (S)-4-¹⁸F-FaML, in addition to antagonism by leucine, valine, and BCH, uptake is strongly antagonized by L-Phe, indicating that although LAT plays a role in cellular uptake, other transport mechanisms may be in operation for these tracers. We then selected a series of ¹⁸F-FBCAAs with varying LAT affinity and examined their biodistribution in mice bearing U-87 cell line xenografts predicted to overexpress LAT (36). We found that accumulation correlated well with LAT affinity trends, with (S)-5-¹⁸F-FHL, (R)-5-¹⁸F-FHL, and (S)-6-¹⁸F-FHHL showing the highest tumor uptake (Fig. 7, Supplemental Table 1) at 60 min after injection. As predicted, (S)-5-¹⁸F-FBAHL showed lesser tumor accumulation and 5-¹⁸F-FPregab, (S)-4-¹⁸F-FαML, and (S)-5-¹⁸F-FαMHL showed a further decrease in tumor accumulation.

Finally, the imaging potential of several ¹⁸F-FBCAAs was examined in a PET study. Dynamic PET images of U-87 tumors in NSG mice at 10 min with (S)-5-¹⁸F-FHL, 5-¹⁸F-FPregab, (S)-4-¹⁸F-FαML, and (S)-5-¹⁸F-FαMHL were obtained and confirmed the results shown in Figure 7. (S)-5-¹⁸F-FHL showed good tumor visualization at 10 min (indicated by orange arrow), whereas the LAT-inactive substrate (S)-5-¹⁸F-FαMHL (LAT affinity $IC_{50} > 1,000 \mu M$) showed no tumor uptake at this time point (Fig. 8). Interestingly, there were notable differences between (S)-4-¹⁸F-FαML and 5-¹⁸F-FPregab (both LAT affinity $IC_{50} > 1,000 \mu M$), as the tumor visualized with (S)-4-¹⁸F-FαML showed much better contrast than that visualized with 5-¹⁸F-FPregab. This finding may be attributable to differences in LAT affinity not revealed by the uptake assay, tumor uptake of (S)-4-¹⁸F-FαML by transporters other than LAT, or differences in (S)-4-¹⁸F-FαML and 5-¹⁸F-FPregab clearance and metabolism.

A closer examination of the *in vivo* behavior of (S)-5-¹⁸F-FHL showed rapid tumor uptake, plateauing at around 10 min and then remaining stable until 30 min of acquisition time, as evidenced by time-activity curves (Fig. 9). The average values of last time frames (uptake values at plateau, i.e., %ID/g, ~ 7.4) corresponded well to the total averages for dynamic scans (at 30 min).

The tumor and brain uptake of (S)-5-¹⁸F-FHL were similar to that of the clinical LAT radiotracer ¹⁸F-FET. In a previous report, ¹⁸F-FET showed an uptake of 6.37 ± 1.67 %ID/g (colon carcinoma tumor) and 2.17 ± 0.64 %ID/g (brain) at 60 min after injection in tumor-bearing nude mice (9). These values are similar to those obtained with (S)-5-¹⁸F-FHL, which showed uptake of 5.29 ± 0.84 %ID/g (U-87 tumor) and 1.63 ± 0.3 %ID/g (brain) at 60 min after injection.

CONCLUSION

Using a photocatalytic fluorination platform, we were able to rapidly access several fluorinated and radiofluorinated BCAAs. An uptake study in CHO-K1 cells revealed SAR

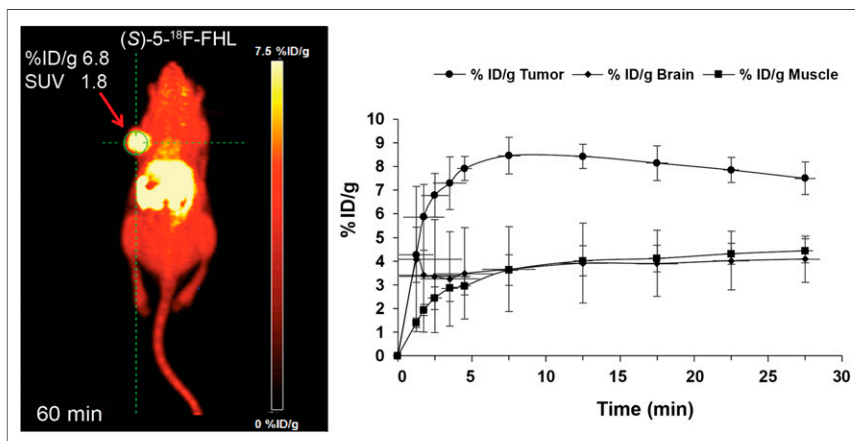


FIGURE 9. (A) *In vivo* dynamic PET imaging of (S)-5-¹⁸F-FHL in NSG mouse bearing U-87 xenograft tumor at 60 min after injection. (B) Time-activity curve of (S)-5-¹⁸F-FHL in tumor, brain, and muscle over 30 min after injection, $n = 3$.

of BCAA uptake by the LAT system and allowed us to select compounds for radiofluorination. A panel of selected ^{18}F -FBCAAs was synthesized, and an *in vitro* competition assay further demonstrated that they are LAT-specific substrates. Further *in vivo* studies confirmed that LAT-mediated uptake in tumor, brain, and other organs correlated with the SAR uncovered in the uptake study. From this study, we were able to identify several promising ^{18}F -FBCAA tracers that will be subjected to further study in models of glioma, prostate cancer, and multiple myeloma.

DISCLOSURE

This work was supported by an NSERC Discovery Grant, an MSFHR Innovation to Commercialization Grant, and a MSFHR Career Investigator Award to Robert Britton, a Hoffmann-La Roche Fellowship (RPF) to Matthew Nodwell, a CIHR Operating Grant and a NSERC CREATE IsoSiM Stipend to Milena Čolović, the BC Leading Edge Endowment Fund to François Bénard, and a Canadian Cancer Society Research Institute Innovation Grant to Paul Schaffer. TRIUMF receives federal funding via a contribution agreement with the National Research Council of Canada. No other potential conflict of interest relevant to this article was reported.

ACKNOWLEDGMENTS

We thank the TRIUMF TR13 cyclotron team, in particular David Prevost, Linda Graham, and Samuel Varah.

REFERENCES

- Hanahan D, Weinberg RA. Hallmarks of cancer: the next generation. *Cell*. 2011;144:646–674.
- Hosios AM, Hecht VC, Danai LV, et al. Amino acids rather than glucose account for the majority of cell mass in proliferating mammalian cells. *Dev Cell*. 2016;36:540–549.
- Huang C, McConathy J. Radiolabeled amino acids for oncologic imaging. *J Nucl Med*. 2013;54:1007–1010.
- Shotwell MA, Jayme DW, Kilberg MS, Oxender DL. Neutral amino acid transport systems in Chinese hamster ovary cells. *J Biol Chem*. 1981;256:5422–5427.
- Kanai Y, Segawa H, Miyamoto K, Uchino H, Takeda E, Endou H. Expression cloning and characterization of a transporter for large neutral amino acids activated by the heavy chain of 4F2 antigen (CD98). *J Biol Chem*. 1998;273:23629–23632.
- Wang Q, Holst J. L-type amino acid transport and cancer: targeting the mTORC1 pathway to inhibit neoplasia. *Am J Cancer Res*. 2015;5:1281–1294.
- Boado RJ, Li JY, Nagaya M, Zhang C, Pardridge WM. Selective expression of the large neutral amino acid transporter at the blood-brain barrier. *Proc Natl Acad Sci USA*. 1999;96:12079–12084.
- Roberts LM, Black DS, Raman C, et al. Subcellular localization of transporters along the rat blood-brain barrier and blood-cerebral-spinal fluid barrier by *in vivo* biotinylation. *Neuroscience*. 2008;155:423–438.
- Wester HJ, Herz M, Weber W, et al. Synthesis and radiopharmacology of *O*-(2-[^{18}F]fluoroethyl)-L-tyrosine for tumor imaging. *J Nucl Med*. 1999;40:205–212.
- Chen W, Silverman DH, Delaloye S, et al. ^{18}F -FDOPA PET imaging of brain tumors: comparison study with ^{18}F -FDG PET and evaluation of diagnostic accuracy. *J Nucl Med*. 2006;47:904–911.
- Sai KK, Huang C, Yuan L, et al. ^{18}F -AFETP, ^{18}F -FET, and ^{18}F -FDG imaging of mouse DBT gliomas. *J Nucl Med*. 2013;54:1120–1126.
- Calabria F, Chiaravalloti A, Di Pietro B, Grasso C, Schillaci O. Molecular imaging of brain tumors with ^{18}F -DOPA PET and PET/CT. *Nucl Med Commun*. 2012;33:563–570.

- Inoue T, Shibasaki T, Oriuchi N, et al. ^{18}F alpha-methyl tyrosine PET studies in patients with brain tumors. *J Nucl Med*. 1999;40:399–405.
- Franzius C, Kopka K, van Valen F, et al. Characterization of 3-[^{123}I]iodo-L-alpha-methyl tyrosine ([^{123}I]JMT) transport into human Ewing's sarcoma cells *in vitro*. *Nucl Med Biol*. 2001;28:123–128.
- Wiriyaerkmul P, Nagamori S, Tominaga H, et al. Transport of 3-fluoro-L-alpha-methyl-tyrosine by tumor-upregulated L-type amino acid transporter 1: a cause of the tumor uptake in PET. *J Nucl Med*. 2012;53:1253–1261.
- Kobayashi M, Hashimoto F, Ohe K, et al. Transport mechanism of ^{11}C -labeled L- and D-methionine in human-derived tumor cells. *Nucl Med Biol*. 2012;39:1213–1218.
- Bouhrel A, Alyami W, Li A, Yuan L, Rich K, McConathy J. Effect of alpha-methyl versus alpha-hydrogen substitution on brain availability and tumor imaging properties of heptanoic [F-18]fluoroalkyl amino acids for positron emission tomography (PET). *J Med Chem*. 2016;59:3515–3531.
- Chin BB, McDougald D, Weitzel DH, et al. Synthesis and preliminary evaluation of 5-[^{18}F]fluoro-leucine. *Curr Radiopharm*. 2017;10:41–50.
- Nagamori S, Wiriyaerkmul P, Okuda S, et al. Structure-activity relations of leucine derivatives reveal critical moieties for cellular uptake and activation of mTORC1-mediated signaling. *Amino Acids*. 2016;48:1045–1058.
- Bouhrel A, Zhou D, Li A, Yuan L, Rich KM, McConathy J. Synthesis, radiolabeling, and biological evaluation of (R)- and (S)-2-amino-5-[^{18}F]fluoro-2-methylpentanoic acid ((R)-, (S)-[^{18}F]FAMPe) as potential positron emission tomography tracers for brain tumors. *J Med Chem*. 2015;58:3817–3829.
- Erment J, Coenen HH. Methods for ^{11}C - and ^{18}F -labelling of amino acids and derivatives for positron emission tomography imaging. *J Labelled Comp Radiopharm*. 2013;56:225–236.
- Nodwell MB, Yang H, Čolović M, et al. ^{18}F -fluorination of unactivated C-H bonds in branched aliphatic amino acids: direct synthesis of oncological positron emission tomography imaging agents. *J Am Chem Soc*. 2017;139:3595–3598.
- Chenault H, Dahmer J, Whitesides G. Kinetic resolution of unnatural and rarely occurring amino-acids: enantioselective hydrolysis of N-acyl amino-acids catalyzed by acylase-I. *J Am Chem Soc*. 1989;111:6354–6364.
- Halperin SD, Fan H, Chang S, Martin RE, Britton R. A convenient photocatalytic fluorination of unactivated C-H bonds. *Angew Chem Int Ed Engl*. 2014;53:4690–4693.
- Halperin SD, Kwon D, Holmes M, et al. Development of a direct photocatalytic C-H fluorination for the preparative synthesis of odanacatib. *Org Lett*. 2015;17:5200–5203.
- Nodwell MB, Bagai A, Halperin SD, Martin RE, Knust H, Britton R. Direct photocatalytic fluorination of benzylic C-H bonds with N-fluorobenzenesulfonimide. *Chem Commun Camb*. 2015;51:11783–11786.
- Geier EG, Schlessinger A, Fan H, et al. Structure-based ligand discovery for the large-neutral amino acid transporter 1, LAT-1. *Proc Natl Acad Sci USA*. 2013;110:5480–5485.
- Teare H, Robins EG, Arstad E, Luthra SK, Gouverneur V. Synthesis and reactivity of [^{18}F]-N-fluorobenzenesulfonimide. *Chem Commun (Camb)*. 2007:2330–2332.
- Turjanski N, Sawle GV, Playford ED, et al. PET studies of the presynaptic and postsynaptic dopaminergic system in Tourette's syndrome. *J Neurol Neurosurg Psychiatry*. 1994;57:688–692.
- Kim CS, Cho SH, Chun HS, et al. BCH, an inhibitor of system L amino acid transporters, induces apoptosis in cancer cells. *Biol Pharm Bull*. 2008;31:1096–1100.
- Hyde R, Taylor PM, Hundal HS. Amino acid transporters: roles in amino acid sensing and signalling in animal cells. *Biochem J*. 2003;373:1–18.
- Altan B, Kaira K, Watanabe A, et al. Relationship between LAT1 expression and resistance to chemotherapy in pancreatic ductal adenocarcinoma. *Cancer Chemother Pharmacol*. 2018;81:141–153.
- Yuan Z, Nodwell MB, Yang H, et al. Site-selective, late-stage C-H ^{18}F -fluorination on unprotected peptides for positron emission tomography imaging. *Angew Chem Int Ed Engl*. 2018;57:12733–12736.
- Li Z, Taylor CP, Weber M, et al. Pregabalin is a potent and selective ligand for $\alpha_2\delta$ -1 and $\alpha_2\delta$ -2 calcium channel subunits. *Eur J Pharmacol*. 2011;667:80–90.
- Belliotti TR, Capiris T, Ekhatov IV, et al. Structure-activity relationships of pregabalin and analogues that target the alpha₂-delta protein. *J Med Chem*. 2005;48:2294–2307.
- Barretina J, Caponigro G, Stransky N, et al. The cancer cell line encyclopedia enables predictive modelling of anticancer drug sensitivity. *Nature*. 2012;483:603–607.